



Curing epoxy with polyethylene glycol (PEG) surface-functionalized $Ni_xFe_{3-x}O_4$ magnetic nanoparticles

Maryam Jouyandeh^a, Zohre Karami^a, Jagar A. Ali^b, Isa Karimzadeh^c, Mustafa Aghazadeh^a, Fouad Laoutid^d, Henri Vahabi^{e,f}, Mohammad Reza Saeb^{g,*}, Mohammad Reza Ganjali^{a,h,*}, Philippe Dubois^{d,*}

^a Center of Excellence in Electrochemistry, School of Chemistry, College of Science, University of Tehran, Tehran, Iran

^b Department of Petroleum Engineering, Faculty of Engineering, Soran University, Kurdistan Region, Iraq

^c Department of Physics, Bonab Branch, Islamic Azad University, Bonab, Iran

^d Service des Matériaux Polymères et Composites (SMPC), Centre d'Innovation et de Recherche en Matériaux et Polymères (CIRMAP), Université de Mons – UMONS / Materianova, Place du Parc 20, 7000, Mons, Belgium

^e Université de Lorraine, CentraleSupélec, LMOPS, F-57000, Metz, France

^f Laboratoire Matériaux Optiques, Photoniques et Systèmes, CentraleSupélec, Université Paris-Saclay, 57070, Metz, France

^g Department of Resin and Additives, Institute for Color Science and Technology, P.O. Box: 16765-654, Tehran, Iran

^h Biosensor Research Center, Endocrinology and Metabolism Molecular-Cellular Sciences Institute, Tehran University of Medical Sciences, Tehran, Iran

ARTICLE INFO

Keywords:

Cure Index

Epoxy

Nanoparticles

Bulk modification

Tunable cross-link density

ABSTRACT

Properties of thermoset nanocomposites are dependent on cross-link density of resin network. Surface modification was known as the main solution to nanoparticle aggregation problem. Although surface modification can assist in reaction between curing moieties, tuning cross-link density of network remains as a challenge for desired properties. In this work, naked, polyethylene glycol (PEG)-capped (surface modified) and Ni^{2+} -doped PEG-capped (surface-bulk modified) magnetic iron oxide (MIO) nanoparticles were synthesized via cathodic electrodeposition, and then characterized by X-ray diffraction, field-emission scanning electron microscopy, vibrating sample magnetometry and Fourier transform infrared spectroscopy. Low filled epoxy nanocomposites containing 0.1 wt.% of three aforementioned MIOs were prepared and underwent dynamic differential scanning calorimetry (DSC). The quality of cure of nanocomposites was studied by *Cure Index* criterion. Applying different heating rates in DSC analyses uncovered the role of bulk and surface-bulk treatment of MIO, by which first steps were taken toward development of epoxy nanocomposites with tunable cross-link density.

1. Introduction

Epoxy nanocomposites have taken credit over years for their high performance features in superadhesives [1,2], anti-corrosion coatings [3,4], medical scaffolds/platforms/implants [5,6], and aerospace devices/elements [7,8]. Nevertheless, epoxy systems containing nanoparticles are prone to thermal and mechanical failure as a consequence of inadequate cross-link density of resin network. Magnetic iron oxide (MIO) nanoparticles are well-known for their extraordinary potential for removal of pollutants from wastewater [9,10], detection of carbohydrates [11,12], and good features in hyperthermia treatments and MRI imaging in medicine [13–15]. They have occasionally been considered in development of coatings, but their very low potential for

curing with epoxy resin has been recognized in a series of previous studies [16]. There have also been attempts to synthesis and functionalization of MIOs for improvement of their curing ability [17–19]. A comparative study revealed dependency of epoxy curing on surface modification of MIOs [20–22]. Nevertheless, the effect of bulk modification of MIOs in addition to surface functionalization on enhancement of cross-link density of epoxy/MIO nanocomposites was not reported yet.

In contrast to various chemical methods such as thermal decomposition, co-precipitation, sol-gel, and hydrothermal procedures used in synthesis of MIOs with a very low level of control over particle size, one-pot electrochemical synthesis by cathodic electrodeposition (CED) via basic electro-generation appeared a facile route to prepare well-

* Corresponding author at: Center of Excellence in Electrochemistry, School of Chemistry, College of Science, University of Tehran, Tehran, Iran. & Department of Resin and Additives, Institute for Color Science and Technology, P.O. Box: 16765-654, Tehran, Iran. & Service des Matériaux Polymères et Composites (SMPC), Centre d'Innovation et de Recherche en Matériaux et Polymères (CIRMAP), Université de Mons – UMONS/ Materianova, Place du Parc 20, 7000, Mons, Belgium.

E-mail addresses: saeb-mr@icrc.ac.ir (M.R. Saeb), ganjali@ut.ac.ir (M.R. Ganjali), philippe.dubois@umons.ac.be (P. Dubois).

<https://doi.org/10.1016/j.porgcoat.2019.105250>

Received 11 July 2019; Received in revised form 19 July 2019; Accepted 22 July 2019

Available online 19 August 2019

0300-9440/© 2019 Elsevier B.V. All rights reserved.

crystallized pure MIO nanoparticles in both naked and surface coated forms [23,24]. Having responded uniform particle size requirement, CED method was brilliant for synthesizing metal cations doped (M^{n+} -doped) MIOs at mild conditions [25], so that $M = Co^{2+}$ [26], La^{3+} [27], Bi^{2+} [28], Zn^{2+} [29] and Dy^{3+} [30] were precisely synthesized. Such a possibility can be considered in bulk and surface engineering of MIOs for efficient epoxy curing.

In this work, three types of MIOs including naked, PEG-capped and PEG- Ni^{2+} -doped MIOs were prepared through one-step CED method. The synthesized MIOs were then analyzed by field-emission scanning electron microscopy (FE-SEM), Fourier-transform infrared spectrophotometry (FTIR), X-ray diffraction (XRD) and vibrating sample magnetometry (VSM) techniques. The curability of epoxy in the presence of PEG-capped MIO and PEG- Ni^{2+} -doped MIO was investigated by dynamic differential scanning calorimetry (DSC) at different heating rates of 5, 10, 15, and 20 °C/min in terms of *Cure Index*.

2. Experimental

2.1. Materials

$Fe(NO_3)_3 \cdot 9H_2O$ (Sigma-Aldrich, 99.9%), $FeCl_2 \cdot 4H_2O$ (Sigma-Aldrich, 99.5%), $Ni(NO_3)_2 \cdot 4H_2O$ (Sigma-Aldrich, 99.8%) and polyethylene glycol (PEG, Sigma-Aldrich,) were purchased and used without further purification. Furthermore, the epoxy resin (DGEBA) with epoxide equivalent weight of 185–192 g/eq and triethylenetetramine (TETA) with hydrogen equivalent weight of 25 g/eq as a hardener were supplied from Hexion Co.

2.2. Synthesis of MIO samples

The cathodic electrochemical synthesis was used to produce naked-, PEG-capped- and Ni^{2+} -doped magnetic iron oxide nanoparticles. The electrochemical set-up and condition reported in Ref. [31], was applied here to synthesize the MIO samples. Briefly, the electrochemical cell was constructed using a steel 316 L cathode ($SA = 100\text{cm}^2$) centered between two graphite anodes with SA of 100cm^2 immersed into the deposition electrolyte and connected to an external power supply by Cu wires. The applied electrochemical conditions were $T_{\text{bath}} = 25\text{ }^\circ\text{C}$, $t_{\text{synthesis}} = 30\text{ min}$ and $i = 10\text{ mA cm}^{-2}$. Only bath composition was different in the synthesis of MIO samples, which includes; in the case of naked-MIO deposition: 2 g $Fe(NO_3)_3 \cdot 9H_2O$ + 1 g $FeCl_2 \cdot 4H_2O$ dissolved in one liter distilled H_2O , for synthesis of PEG-capped MIO sample: 2 g $Fe(NO_3)_3 \cdot 9H_2O$ + 1 g $FeCl_2 \cdot 4H_2O$ + 1 g PEG dissolved in one liter distilled H_2O and in the synthesis of PEG/ Ni^{2+} -doped MIO: 2 g $Fe(NO_3)_3 \cdot 9H_2O$ + 1 g $FeCl_2 \cdot 4H_2O$ + 0.3 g $Ni(NO_3)_2 \cdot 4H_2O$ + 1 g PEG dissolved in 1 liter distilled water. For synthesis of these three MIO samples, the electrodeposition experiment was carried out for 30 min at the above mentioned conditions. As the deposition run was stopped, black films had formed on the steel cathode in all three mentioned baths. The following steps were then performed to obtain dry MIO powders; (1) the cathodes were removed from the deposition bath and were washed with water several times and the deposited films were collected from the steel cathode surface, (2) the obtained wet powders were repeatedly washed with water, and (3) were then heated at 70 °C for 1 h. After these steps, the black dried powders were obtained, which were labeled naked-MIO, PEG capped-MIO and PEG/ Ni^{2+} -doped MIO. The atomic view of capping and doping process is shown in Fig. 1.

2.3. Epoxy nanocomposites preparation

The preparation of epoxy nanocomposite consists of 0.1 wt.% of naked MIO, PEG capped MIO and PEG/ Ni^{2+} -doped MIO nanoparticle was done by below steps: nanoparticles were dispersed in epoxy resin

by sonication with 50% duty cycle for 5 min. Then, for achieving finer dispersion the nanocomposite was mixed with a mechanical mixer at 2500 rpm for 20 min. Finally, epoxy stoichiometric amount of TETA (100:13) was added to epoxy resin, thoroughly (Table 1).

2.4. Characterization

Morphological features of the deposited MIO samples were observed using an FE-SEM microscope, Model; Mira 3-XMU and accelerating voltage of 100 kV. FT-IR spectra were recorded through Bruker Vector 22 IR spectrometer in the frequency range of $4000\text{--}400\text{ cm}^{-1}$. XRD patterns of the fabricated MIO samples were provided by PW-1800 X-ray diffraction with a Co K α radiation. Magnetic behaviors of the fabricated MIO particles were also specified in the range of -20000 Oe to 20000 Oe at RT condition using a VSM instrument, model: lakeshore 7400.

Differential scanning calorimetry (DSC) was performed on Perkin Elmer DSC 4000 to study the cure state of the neat epoxy and its nanocomposites including 0.1 wt.% of PEG capped MIO and PEG/ Ni^{2+} -doped MIO under nonisothermal conditions. Dynamic DSCs were carried out at different heating rates (β) of 5, 10, 15, 20 °C min^{-1} over a temperature range of 25–200 °C under nitrogen with the flow rate of 20 $\text{mL} \cdot \text{min}^{-1}$.

3. Results and discussion

3.1. Structure and morphology

The XRD patterns of the deposited MIO samples are given in Fig. 2. The observed diffraction in these patterns could be assigned as crystal planes of (111), (220), (311), (400), (422), (511), (440), and (533), which all these peaks are in good agreement with those reported to MIO with pure magnetite crystal structure (JCPDS number of 01-074-1910) [27–31]. In fact, these XRD patterns are well matched with those reported for pure cubic Fe_3O_4 . Through the Debye–Sherrer equation ($D = K\lambda/\beta\cos\theta$), average crystallite sizes (D) of 7.1 nm (provided from Ref. [31]), 14.7 nm and 15.6 nm were calculate for naked-MIO, PEG-capped MIO and PEG/ Ni^{2+} -doped MIO, respectively.

Morphological characteristics of the synthesized MIO samples were characterized through FE-SEM observations and shown in Fig. 3. For all deposited MIO powders, spherical particles with an average diameter of 20 nm are observed in the FE-images.

The FT-IR spectra for the MNPs powders are presented in Fig. 4. In all spectra, the IR bands located at $425\text{--}430\text{ cm}^{-1}$ and $585\text{--}588\text{ cm}^{-1}$ can be assigned to the stretching vibration modes of $Fe^{2+}\text{--O--Ni}^{2+}$ and $Fe^{3+}\text{--O--Fe}^{2+}$ bonds [31–33]. For both PEG-capped MIO and PEG/ Ni^{2+} -doped MIO samples in Fig. 3b and c, various IR bands are observed in the range of $700\text{ cm}^{-1}\text{--}3000\text{ cm}^{-1}$, which could be related to the following IR bands [33–35]; (i) $\nu_{\text{stretching}}$ of C–H at $2930\text{--}2935\text{ cm}^{-1}$ and $2875\text{--}2880\text{ cm}^{-1}$, $\nu_{\text{stretching}}$ of CH_2 at $1465\text{--}1470\text{ cm}^{-1}$ and $1375\text{--}1380\text{ cm}^{-1}$, $\nu_{\text{stretching}}$ and ν_{bending} of C–O–C bonds at $1280\text{--}1285\text{ cm}^{-1}$ and $1165\text{--}1670\text{ cm}^{-1}$, ν_{wagging} of C–H at $880\text{--}890\text{ cm}^{-1}$, $\nu_{\text{stretching}}$ of C–C bond at $1130\text{--}1135\text{ cm}^{-1}$ and $\nu_{\text{stretching}}$ of C–O–H bond at $1055\text{--}1160\text{ cm}^{-1}$. These IR data verified the PEG-capped features for both PEG/MIO and PEG/ Ni^{2+} -doped MIO samples.

Fig. 5 shows the VSM curves for the synthesized MIO powders. The VSM profiles of all three MNPs exhibited a complete S shape and hence their superparamagnetic behaviors. From Fig. 5, the saturation magnetization (M_s), remanence (M_r) and coercivity (C_e) values were measured to be $M_s = 72.96\text{ emu/g}$, $M_r = 0.95\text{ emu/g}$ and $C_e = 2.9\text{ Oe}$ (for naked-MIO as reported in Ref. [31]), $M_s = 49.52\text{ emu/g}$, $M_r = 0.72\text{ emu/g}$ and $C_e = 1.45\text{ Oe}$ (for PEG/MIO) and $M_s = 34.65\text{ emu/g}$, $M_r = 0.59\text{ emu/g}$ and $C_e = 1.17\text{ Oe}$ (for PEG/ Ni^{2+} -

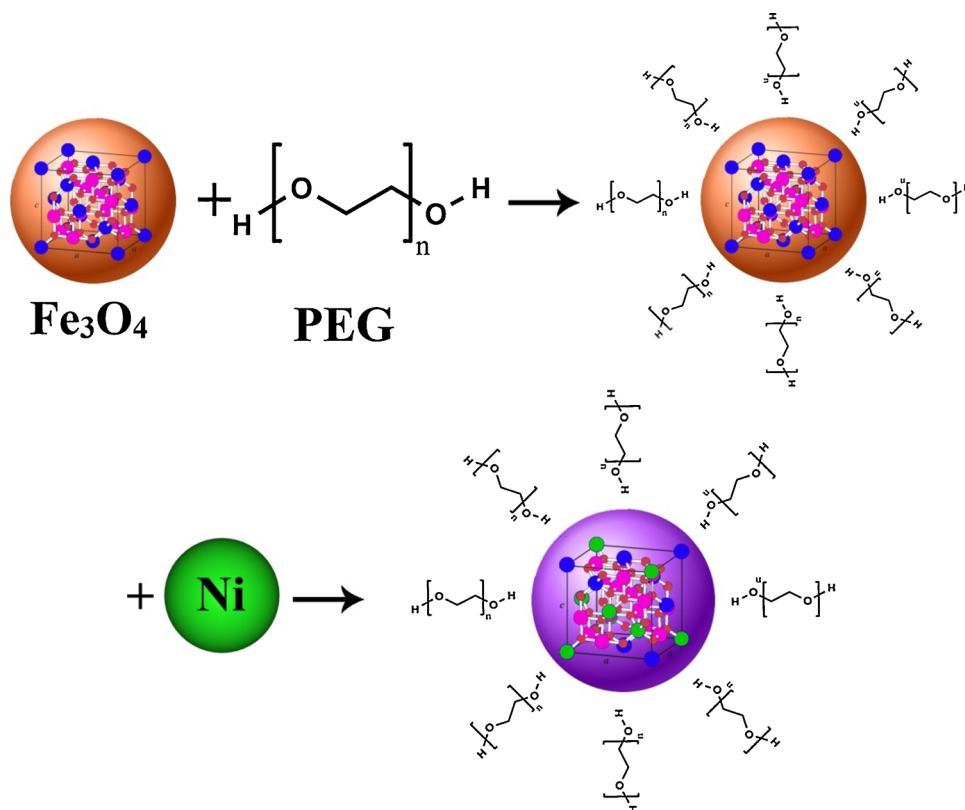


Fig. 1. PEG capping and Ni²⁺ doping of MIO.

Table 1

Weight composition of the prepared nanocomposites.

Sample code	Nanoparticle	Content (wt. %)
EP	–	0.0
EP/MIO	MIO	0.1
EP/PEG capped MIO	PEG capped MIO	0.1
EP/PEG-Ni ²⁺ -doped MIO	PEG/Ni ²⁺ -doped MIO	0.1

doped MIO). These magnetic data proved the superparamagnetic behavior for all the synthesized MIO samples and also verified an improvement in the magnetic characters of MIO powder due to the PEG-

capping and Ni-doping processes.

3.2. Cure labeling of epoxy nanocomposites

It is well-known that ultimate properties of thermoset systems are pertinent to the degree of crosslinking at the presence of filler in the matrix [36–40]. Therefore, the missing ring in properties-microstructure-relationship of thermoset composite is studying of curing reaction. In this study, the effect of PEG-capped MIO and PEG/Ni²⁺-doped MIO nanoparticles on curing of epoxy was studied at the heating rates (β) of 5, 10, 15 and 20 °C/min by nonisothermal DSC (Fig. 6). Moreover, the peak temperature, the initial and final cure temperature

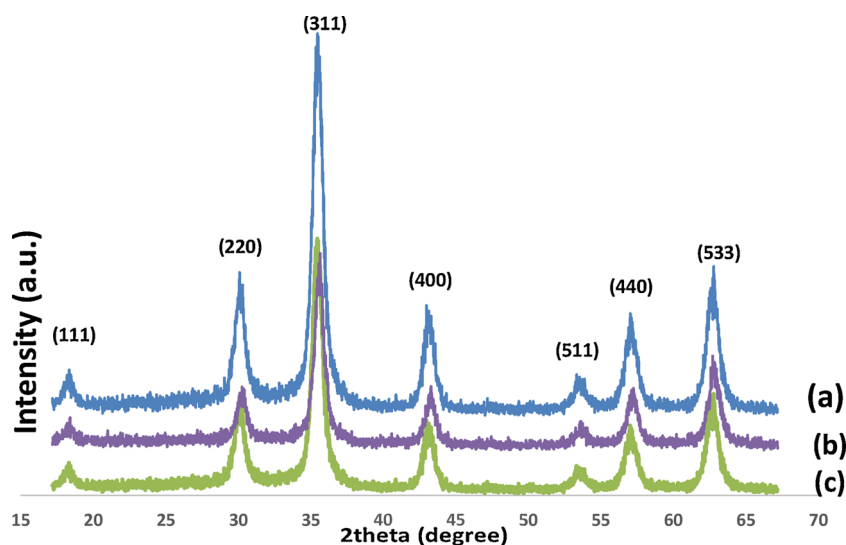


Fig. 2. XRD patterns of the synthesized MIO samples, (a) naked-MIOs, (b) PEG-capped MIO and (c) PEG/Ni²⁺-doped MIO.

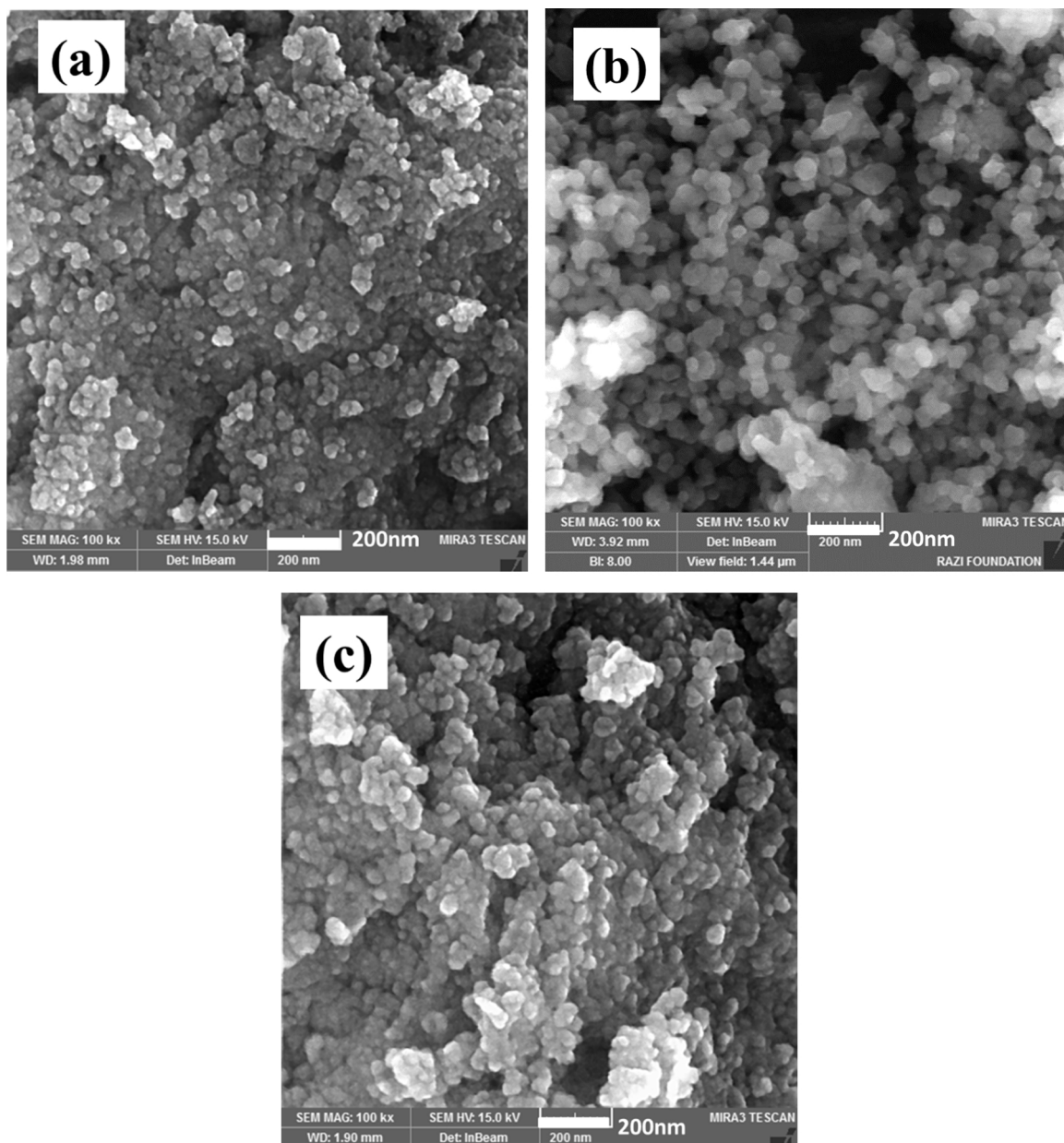


Fig. 3. FE-SEM images of naked-MIO [31], (b) PEG-capped MIO and (c) PEG/Ni²⁺-doped MIO.

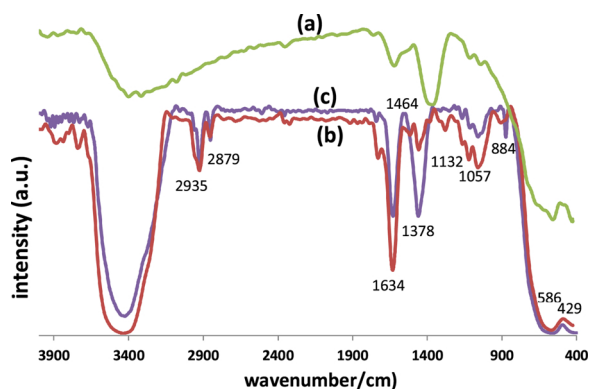


Fig. 4. FT-IR spectra of the synthesized (a) naked-MIO, (b) PEG-capped MIO and (c) PEG/Ni²⁺-doped MIO.

(T_p , T_{onset} and T_{endset} , respectively), heat of cure reaction (ΔH) which is calculated as the total area under the exothermic peak, cure temperature range (ΔT) were extracted from the DSC thermograms for neat epoxy and its nanocomposites to estimate ΔT^* ($\Delta T_{nanocomposite} / \Delta T_{neat epoxy}$), ΔH^* ($\Delta H_{nanocomposite} / \Delta H_{neat epoxy}$) and the *Cure Index* ($\Delta T^* \times \Delta H^*$) and reported in (Table 2) [41].

As can be observed in Table 2, T_{onset} of EP/MIO shifted to higher temperatures compared to EP sample because of the steric hindrance effect of MIO, which led to the viscosity build up [42]. In addition, as shown in Fig. 6, addition of PEG capped MIO and PEG-Ni²⁺-doped MIO nanoparticles shifted DSC thermograms to higher temperature and enlarged cure temperature range. OH groups of PEG on the surface of nanoparticles participate at epoxide ring opening and signify the autocatalytic nature of epoxy curing reaction at higher temperature which results in increase of T_p and T_{endset} [43,44]. The values of epoxy/amine heat of cure increased by addition of PEG capped MIO and PEG-Ni²⁺-doped MIO compared to EP/NIO nanocomposites at all heating rates. This improvement in ΔH indicated that by anchoring PEG

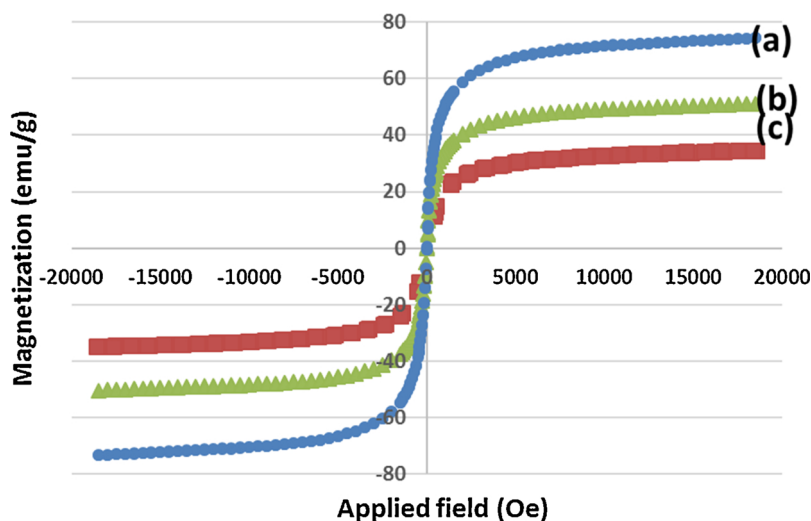


Fig. 5. VSM curves of the fabricated (a) naked-MIO [31], (b) PEG-capped MIO and (c) PEG/ Ni^{2+} -doped MIO.

macromolecules on the surface of MIO decrease the hindering effect of naked MIO. The mobility and diffusion of PEG macromolecules allow the hydroxyl end-groups to reach and react with epoxy groups remaining unreacted within the cross-linking epoxy/amine networks. In fact, PEG on the surface of MIO and Ni^{2+} -doped MIO facilitated curing reaction of epoxy in late stage of cure when the reaction is under diffusion control [45]. The reaction of epoxy with PEG- Ni^{2+} -doped MIO

nanoparticles is shown in Fig. 7. The hydroxyl groups of PEG on the surface of nanoparticles can participate in the curing reaction of epoxy. Since the reaction rate of the OH groups with epoxy is slower than the reaction rate between epoxy and amine groups of hardener, the former reaction occurs at higher temperatures and lead to wider temperature window [46].

Ni dopants only tend to locate in the top layer of MIO crystal.

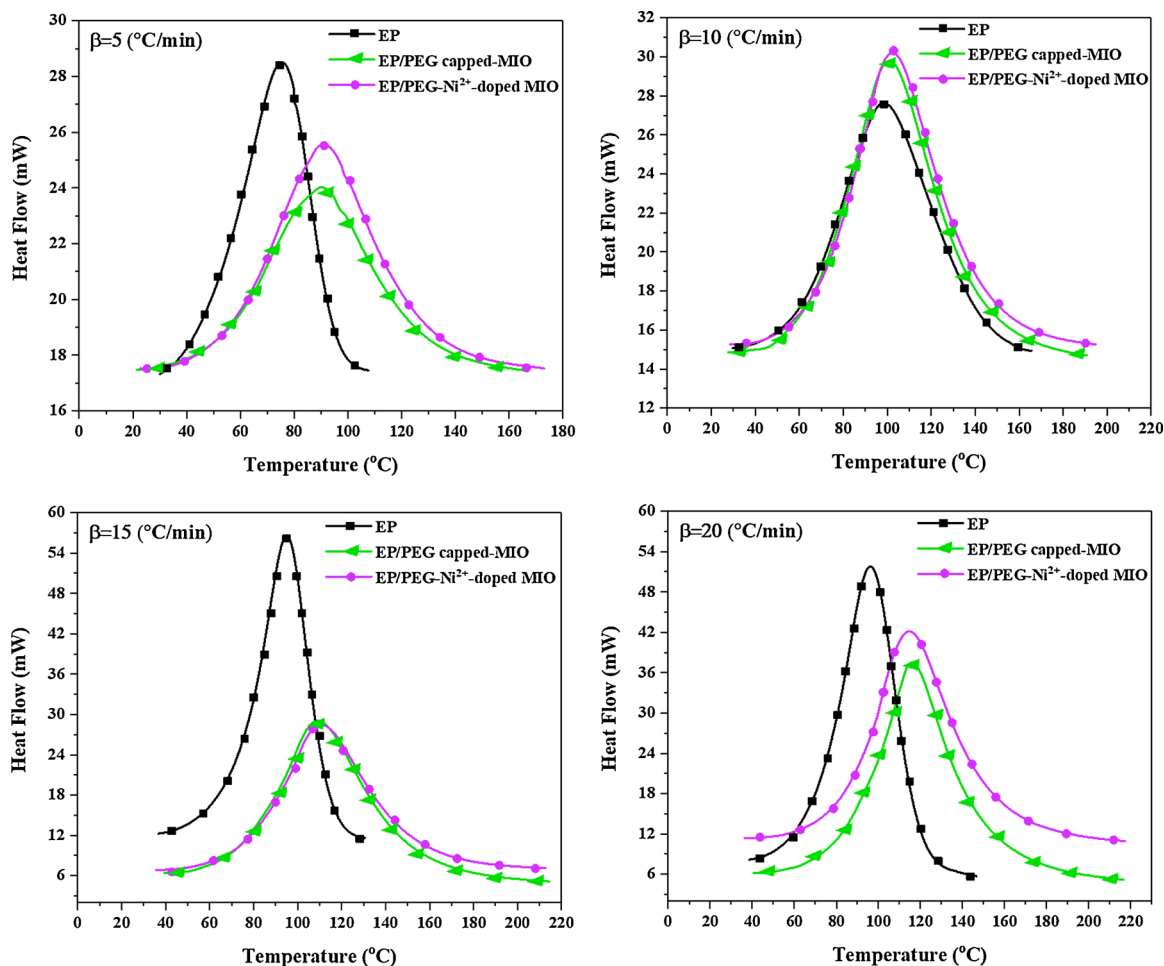


Fig. 6. Dynamic DSC thermograms of EP, EP/PEG capped MIO and EP/PEG- Ni^{2+} -doped MIO at different heating rates.

Table 2
Cure characteristics of the prepared epoxy nanocomposites as a function of heating rate.

Designation	β (°C/min)	T_{onset} (°C)	T_{endset} (°C)	T_p (°C)	ΔT (°C)	ΔH_{∞} (J/g)	ΔT^*	ΔH^*	<i>CI</i>
EP	5	30.04	107.62	75.31	77.58	340.41	n.a.	n.a.	n.a.
	10	29.7	165.3	98.4	135.7	319.40	n.a.	n.a.	n.a.
	15	36.64	191.89	107.89	155.25	377.61	n.a.	n.a.	n.a.
	20	38.62	146.67	96.09	108.05	374.39	n.a.	n.a.	n.a.
^a EP/MIO	5	40.7	140.4	90.3	99.6	186.6	0.83	0.55	0.45
	10	40.7	166.0	99.1	125.3	310.8	0.92	0.97	0.90
	15	46.1	174.4	113.0	128.3	127.7	0.83	0.34	0.28
	20	46.9	191.5	118.0	144.7	164.3	0.90	0.44	0.40
EP/PEG capped MIO	5	21.44	166.70	90.15	145.26	324.30	1.87	0.95	1.77
	10	27.66	190.83	100.86	163.17	378.49	1.20	1.19	1.42
	15	39.42	214.46	109.23	175.04	395.92	1.13	1.05	1.18
	20	40.57	216.58	115.94	176.01	372.16	1.63	0.99	1.61
EP/PEG-Ni ²⁺ -doped MIO	5	22.77	173.03	91.45	150.26	385.18	1.94	1.13	2.19
	10	28.50	194.84	102.37	166.34	371.62	1.23	1.16	1.43
	15	35.65	212.90	110.97	177.25	367.98	1.14	0.97	1.10
	20	36.31	217.33	114.71	181.02	384.30	1.67	1.02	1.70

n.a. – not applicable (reference measurements). Values of the *CI* written in italic shape are indicative of *Goodcure*.

^a Values of the *CI* for this group are *Poor* irrespective of hearing regime.

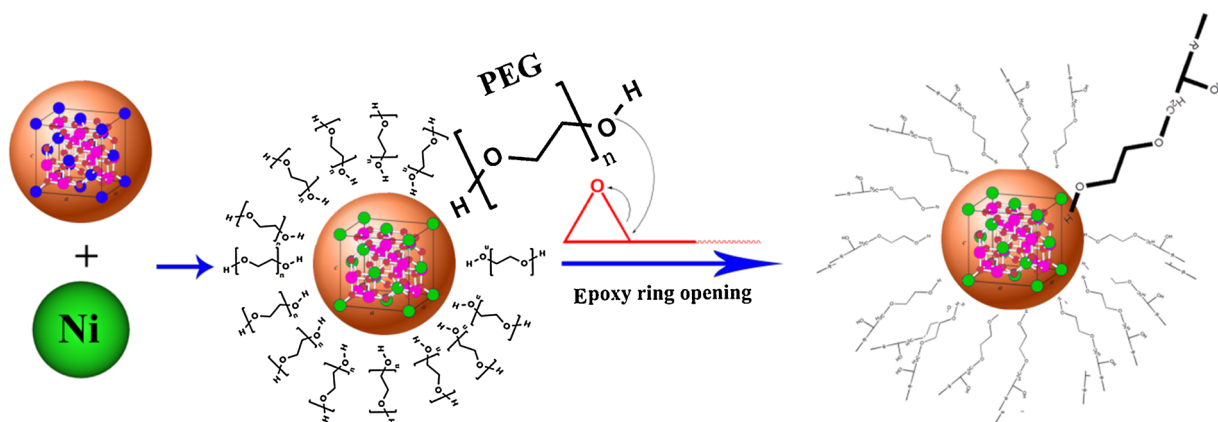


Fig. 7. Possible reaction of PEG-Ni²⁺-doped MIO with epoxy.

Therefore, addition of Ni dopant can dramatically increase active sites on the surface of MIO [32]. By increasing the activity of the surface the number of PEG macromolecules anchored to Ni²⁺-doped MIO may increase. It means that by changing the bulk of nanoparticles it is possible to change the amount of surface functionalization. Accordingly, PEG-Ni²⁺-doped MIO nanoparticles increase enthalpy of cure

compared to neat epoxy and MIO incorporated epoxy at low and high heating rates.

The cure state of epoxy containing 0.1 wt.% of PEG capped MIO and PEG-Ni²⁺-doped MIO at different heating rates based on *CI* is shown in Fig. 8 by plotting ΔH^* versus ΔT^* . Fig. 8 shows three regions: *Excellent cure* ($\Delta T^* < CI < \Delta H^*$, green part), *Good cure* ($CI > \Delta H^*$, blue part)

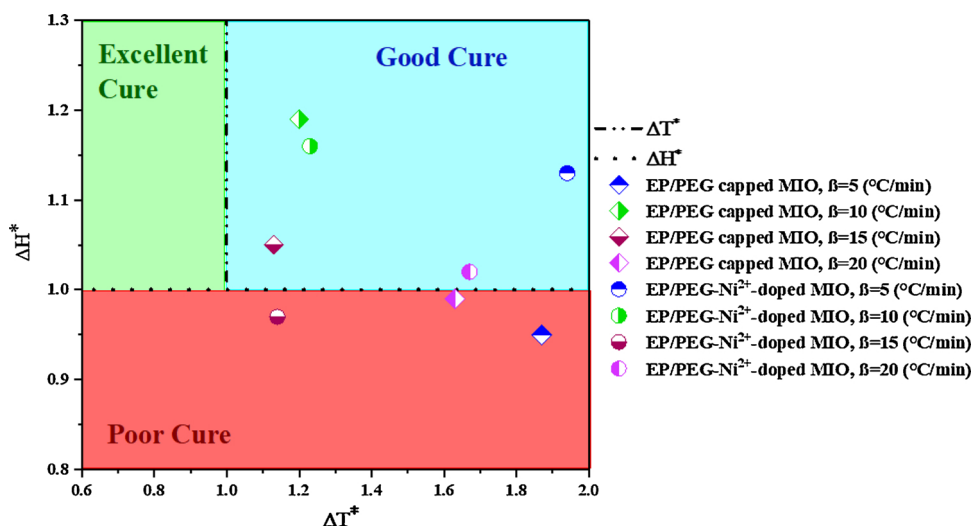


Fig. 8. Cure situation of EP/PEG capped MIO and EP/PEG-Ni²⁺-doped MIO nanocomposites at heating rates of 5, 10, 15 and 20 °C/min.

and *Poor* cure ($CI < \Delta T^*$, red part) [47]. It is evident that from Fig. 8 EP/PEG capped MIO and EP/PEG-Ni²⁺-doped MIO at heating rate of 5, 10 and 20 °C/min *CI* shows *Good* cure whereas at heating rate of 15 °C/min *CI* is in *Poor* region.

As can be observed, ΔH^* values of EP/PEG/Ni²⁺-doped MIO are higher than EP/PEG-capped MIO, which can be inferred by the obtained data from VSM analysis. In fact, naked MIO has high surface area/volume ratios and a high tendency to agglomerate and reduce surface energies. Agglomeration of MIOs can reduce their role in epoxy crosslinking. However, surface modification of MIO by PEG and Ni-doping of it prevent agglomeration of nanoparticles in epoxy matrix which could be proved by VSM data. Lower *Ms* and *Mr* values observed for PEG/Ni²⁺-doped MIO in VSM data indicate single domain centers for nanoparticles. Hence, it is expected that PEG/Ni²⁺-doped MIO exhibit better contribution into the epoxy crosslinking as compared with PEG-capped MIO.

At low heating rate, PEG-capped MIO could not efficiently participate in epoxide ring opening due to the inadequate kinetic energy per molecule. In addition, introducing PEG-capped MIO in to the epoxy matrix increases the viscosity of the system, which leads to rapid occurrence of gelation and vitrification, as signaled by *Poor* cure state [20]. At high heating rate, PEG chains present on the surface of MIO obtain adequate kinetics energy but in a low time interval which led to *Poor* cure state. At medium heating rates, PEG-capped MIO may receive enough energy and acts strong role in catalyzing epoxide ring opening that changed cure state from *Poor* to *Good* [48]. In the case of PEG/Ni²⁺-doped MIO incorporated epoxy system at heating rate of 15 °C/min, beside to the increase in viscosity, functional groups anchored to the surface of PEG/Ni²⁺-doped MIO don't have enough time to participate in curing reaction of epoxy. Therefore, in this heating rate, cure state of the system is *Poor*.

4. Conclusion

MIO, PEG capped MIO and EP/PEG-Ni²⁺-doped MIO nanoparticles were synthesized electrochemically and fully characterized by FTIR, XRD, FESEM and VSM analyses. XRD results indicated that the average crystallite size of the 14.7 nm and 15.6 nm were obtained for naked-MIO, PEG-capped MIO and PEG/Ni²⁺-doped MIO, respectively. VSM data proved the superparamagnetic behavior for all the synthesized MIO samples and also verified an improvement in the magnetic characters of MIO powder due to the PEG-capping and Ni-doping processes. Epoxy-based nanocomposites were prepared by introducing 1 wt.% of PEG-capped MIO and PEG/Ni²⁺-doped MI into the epoxy and their curing reaction was discussed using dynamic DSC. From VSM results the values of *Ms* = 49.52 emu/g, *Mr* = 0.72 emu/g were obtained for PEG/MIO and *Ms* = 34.65 emu/g, *Mr* = 0.59 emu/g for PEG/Ni²⁺-doped MIO. Observation of lower *Ms* and *Mr* values for PEG/Ni²⁺-doped MIO exhibited better dispersion of this nanoparticle compared to PEG/MIO which resulted in higher impact of PEG/Ni²⁺-doped MIO on the epoxy crosslinking. Therefore, the shift in cure state from *Poor* to *Good* was observed for EP/PEG/Ni²⁺-doped MIO system at heating rates of 5 and 20 °C/min. These results smooth the way towards curing tunable epoxy nanocomposites for advanced applications.

References

- M. Jouyandeh, O. Moini Jazani, A.H. Navarchian, M.R. Saeb, High-performance epoxy-based adhesives reinforced with alumina and silica for carbon fiber composite/steel bonded joints, *J. Reinf. Plast. Compos.* 35 (2016) 1685–1695.
- M. Jouyandeh, O.M. Jazani, A.H. Navarchian, M. Shabanian, H. Vahabi, M.R. Saeb, Bushy-surface hybrid nanoparticles for developing epoxy superadhesives, *Appl. Surf. Sci.* 479 (2019) 1148–1160.
- B. Ramezanzadeh, G. Bahlakeh, M. Ramezanzadeh, Polyaniline-cerium oxide (PANI-CeO₂) coated graphene oxide for enhancement of epoxy coating corrosion protection performance on mild steel, *Corros. Sci.* 137 (2018) 111–126.
- T.A. Truc, T.T. Thuy, V.K. Oanh, T.T.X. Hang, A.S. Nguyen, N. Caussé, N. Pèbère, 8-hydroxyquinoline-modified clay incorporated in an epoxy coating for the corrosion protection of carbon steel, *Surf. Interfaces* 14 (2019) 26–33.
- S. Barua, P. Chattopadhyay, L. Aidew, A.K. Buragohain, N. Karak, Infection-resistant hyperbranched epoxy nanocomposite as a scaffold for skin tissue regeneration, *Polym. Int.* 64 (2015) 303–311.
- S. Barua, B. Gogoi, L. Aidew, A.K. Buragohain, P. Chattopadhyay, N. Karak, Sustainable resource based hyperbranched epoxy nanocomposite as an infection resistant, biodegradable, implantable muscle scaffold, *ACS Sustain. Chem. Eng.* 3 (2015) 1136–1144.
- J. Njuguna, K. Pieliowski, Polymer nanocomposites for aerospace applications: properties, *Adv. Eng. Mater.* 5 (2003) 769–778.
- J. Njuguna, K. Pieliowski, J. Fan, Polymer nanocomposites for aerospace applications, *Advances in Polymer Nanocomposites*, Elsevier, 2012, pp. 472–539.
- J.-F. Liu, Z.-s. Zhao, G.-b. Jiang, Coating Fe₃O₄ magnetic nanoparticles with humic acid for high efficient removal of heavy metals in water, *Environ. Sci. Technol.* 42 (2008) 6949–6954.
- Y. Shen, J. Tang, Z. Nie, Y. Wang, Y. Ren, L. Zuo, Preparation and application of magnetic Fe₃O₄ nanoparticles for wastewater purification, *Sep. Purif. Technol.* 68 (2009) 312–319.
- H. Wei, E. Wang, Fe₃O₄ magnetic nanoparticles as peroxidase mimetics and their applications in H₂O₂ and glucose detection, *Anal. Chem.* 80 (2008) 2250–2254.
- M. Hosseini, F. Sadat Sabet, H. Khabbaz, M. Aghazadeh, F. Mizani, M.R. Ganjali, Enhancement of the peroxidase-like activity of cerium-doped ferrite nanoparticles for colorimetric detection of H₂O₂ and glucose, *Anal. Methods* 9 (2017) 3519–3524.
- M. Latorre, C. Rinaldi, Applications of magnetic nanoparticles in medicine: magnetic fluid hyperthermia, *P. R. Health Sci. J.* 28 (2009).
- C. Sun, J.S. Lee, M. Zhang, Magnetic nanoparticles in MR imaging and drug delivery, *Adv. Drug Deliv. Rev.* 60 (2008) 1252–1265.
- M. Saeedi, O. Vahidi, V. Goodarzi, M.R. Saeb, L. Izadi, M. Mozafari, A new prospect in magnetic nanoparticle-based cancer therapy: taking credit from mathematical tissue-mimicking phantom brain models, *Nanomed.: Nanotechnol. Biol. Med.* 13 (2017) 2405–2414.
- M.R. Saeb, H. Rastin, M. Shabanian, M. Ghaffari, G. Bahlakeh, Cure kinetics of epoxy/ β -cyclodextrin-functionalized Fe₃O₄ nanocomposites: experimental analysis, mathematical modeling, and molecular dynamics simulation, *Prog. Org. Coat.* 110 (2017) 172–181.
- A.H. Lu, Ee.L. Salabas, F. Schüth, Magnetic nanoparticles: synthesis, protection, functionalization, and application, *Angew. Chemie Int. Ed.* 46 (2007) 1222–1244.
- M. Jouyandeh, N. Rahmati, E. Movahedifar, B.S. Hadavand, Z. Karami, M. Ghaffari, P. Taheri, E. Bakhshandeh, H. Vahabi, M.R. Ganjali, Properties of nano-Fe₃O₄ incorporated epoxy coatings from Cure Index perspective, *Prog. Org. Coat.* 133 (2019) 220–228.
- M.R. Saeb, M. Nonahal, H. Rastin, M. Shabanian, M. Ghaffari, G. Bahlakeh, S. Ghiyasi, H.A. Khonakdar, V. Goodarzi, D. Puglia, Calorimetric analysis and molecular dynamics simulation of cure kinetics of epoxy/chitosan-modified Fe₃O₄ nanocomposites, *Prog. Org. Coat.* 112 (2017) 176–186.
- M. Jouyandeh, S.M.R. Paran, M. Shabanian, S. Ghiyasi, H. Vahabi, M. Badawi, K. Formela, D. Puglia, M.R. Saeb, Curing behavior of epoxy/Fe₃O₄ nanocomposites: a comparison between the effects of bare Fe₃O₄, Fe₃O₄/SiO₂/chitosan and Fe₃O₄/SiO₂/chitosan/imide/phenylalanine-modified nanofillers, *Prog. Org. Coat.* 123 (2018) 10–19.
- M. Jouyandeh, S.M.R. Paran, A. Jannesari, M.R. Saeb, 'Cure Index' for thermoset composites, *Prog. Org. Coat.* 127 (2019) 429–434.
- M. Jouyandeh, M. Shabanian, M. Khaleghi, S.M.R. Paran, S. Ghiyasi, H. Vahabi, K. Formela, D. Puglia, M.R. Saeb, Acid-aided epoxy-amine curing reaction as reflected in epoxy/Fe₃O₄ nanocomposites: chemistry, mechanism, and fracture behavior, *Prog. Org. Coat.* 125 (2018) 384–392.
- M. Aghazadeh, I. Karimzadeh, M.R. Ganjali, Preparation and characterization of amine- and carboxylic acid-functionalized superparamagnetic iron oxide nanoparticles through a one-step facile electro-synthesis method, *Curr. Nanosci.* 15 (2019) 169–177.
- M. Aghazadeh, One-step cathodic electro-synthesis of surface capped Fe₃O₄ ultra-fine nanoparticles from ethanol medium without using coating agent, *Mater. Lett.* 211 (2018) 225–229.
- M. Aghazadeh, M.R. Ganjali, Samarium-doped Fe₃O₄ nanoparticles with improved magnetic and supercapacitive performance: a novel preparation strategy and characterization, *J. Mater. Sci.* 53 (2018) 295–308.
- M. Aghazadeh, M.R. Ganjali, One-pot electrochemical synthesis and assessment of super-capacitive and super-paramagnetic performances of Co²⁺ doped Fe₃O₄ ultra-fine particles, *J. Mater. Sci. Mater. Electron.* 29 (2018) 2291–2300.
- M. Aghazadeh, I. Karimzadeh, M.R. Ganjali, Improvement of supercapacitive and superparamagnetic capabilities of iron oxide through electrochemically grown La³⁺ doped Fe₃O₄ nanoparticles, *J. Mater. Sci. Mater. Electron.* 28 (2017) 19061–19070.
- M. Aghazadeh, I. Karimzadeh, M.R. Ganjali, Preparation of nano-sized bismuth-doped Fe₃O₄ as an excellent magnetic material for supercapacitor electrodes, *J. Korean Inst. Electr. Electron. Mater. Eng.* 47 (2018) 3026–3036.
- M. Aghazadeh, Zn-doped magnetite nanoparticles: development of novel preparation method and evaluation of magnetic and electrochemical capacitance performances, *J. Mater. Sci. Mater. Electron.* 28 (2017) 18755–18764.
- M. Aghazadeh, M.R. Ganjali, Evaluation of supercapacitive and magnetic properties of Fe₃O₄ nano-particles electrochemically doped with dysprosium cations: development of a novel iron-based electrode, *Ceram. Int.* 44 (2018) 520–529.
- M. Aghazadeh, M.R. Ganjali, One-step electro-synthesis of Ni²⁺ doped magnetite nanoparticles and study of their supercapacitive and superparamagnetic behaviors, *J. Mater. Sci. Mater. Electron.* 29 (2018) 4981–4991.
- M. Aghazadeh, I. Karimzadeh, M.R. Ganjali, A. Behzad, Mn²⁺-doped Fe₃O₄ nanoparticles: a novel preparation method, structural, magnetic and electrochemical

- characterizations, *J. Mater. Sci. Mater. Electron.* 28 (2017) 18121–18129.
- [33] I. Karimzadeh, H.R. Dizaji, M. Aghazadeh, Preparation, characterization and PEGylation of superparamagnetic Fe₃O₄ nanoparticles from ethanol medium via cathodic electrochemical deposition (CED) method, *Mater. Res. Express* 3 (2016) 095022.
- [34] I. Karimzadeh, M. Aghazadeh, T. Doroudi, M. Reza Ganjali, P. Hossein Kolivand, D. Gharailou, Superparamagnetic iron oxide nanoparticles modified with alanine and leucine for biomedical applications: development of a novel efficient preparation method, *Curr. Nanosci.* 13 (2017) 274–280.
- [35] I. Karimzadeh, M. Aghazadeh, M.R. Ganjali, P. Norouzi, S. Shirvani-Arani, T. Doroudi, P.H. Kolivand, S.A. Marashi, D. Gharailou, A novel method for preparation of bare and poly (vinylpyrrolidone) coated superparamagnetic iron oxide nanoparticles for biomedical applications, *Mater. Lett.* 179 (2016) 5–8.
- [36] M. Aliakbari, O.M. Jazani, M. Sohrabian, M. Jouyandeh, M.R. Saeb, Multi-nationality epoxy adhesives on trial for future nanocomposite developments, *Prog. Org. Coat.* 133 (2019) 376–386.
- [37] H. Vahabi, M. Jouyandeh, M. Cochez, R. Khalili, C. Vagner, M. Ferriol, E. Movahedifar, B. Ramezanzadeh, M. Rostami, Z. Ranjbar, B.S. Hadavand, M.R. Saeb, Short-lasting fire in partially and completely cured epoxy coatings containing expandable graphite and halloysite nanotube additives, *Prog. Org. Coat.* 123 (2018) 160–167.
- [38] M. Jouyandeh, O.M. Jazani, A.H. Navarchian, M.R. Saeb, Epoxy coatings physically cured with hydroxyl-contained silica nanospheres and halloysite nanotubes, *Prog. Color, Colorants Coat.* 11 (2018) 199–207.
- [39] M. Saeb, H. Vahabi, M. Jouyandeh, E. Movahedifar, R. Khalili, Epoxy-based flame retardant nanocomposite coatings: comparison between functions of expandable graphite and halloysite nanotubes, *Prog. Color Colorants Coat.* 10 (2017) 245–252.
- [40] Z. Karami, O.M. Jazani, A. Navarchian, M. Saeb, Effect of carbon black content on curing behavior of polysulfide elastomer, *Prog. Color Colorants Coat.* 12 (2018) 103–112.
- [41] M. Jouyandeh, S.M.R. Paran, A. Jannesari, D. Puglia, M.R. Saeb, Protocol for nonisothermal cure analysis of thermoset composites, *Prog. Org. Coat.* 131 (2019) 333–339.
- [42] A. Kondyurin, L.A. Komar, A.L. Svistkov, Combinatory model of curing process in epoxy composite, *Compos. Part B Eng.* 43 (2012) 616–620.
- [43] M. Jouyandeh, Z. Karami, O.M. Jazani, K. Formela, S.M.R. Paran, A. Jannesari, M.R. Saeb, Curing epoxy resin with anhydride in the presence of halloysite nanotubes: the contradictory effects of filler concentration, *Prog. Org. Coat.* 126 (2019) 129–135.
- [44] E. Yarahmadi, K. Didehban, M. Shabaniyan, M.R. Saeb, High-performance starch-modified graphene oxide/epoxy nanocomposite coatings: a glimpse at cure kinetics and fracture behavior, *Prog. Color, Colorants Coat.* 11 (2018) 55–62.
- [45] V. Akbari, F. Najafi, H. Vahabi, M. Jouyandeh, M. Badawi, S. Morisset, M.R. Ganjali, M.R. Saeb, Surface chemistry of halloysite nanotubes controls the curability of low filled epoxy nanocomposites, *Prog. Org. Coat.* 135 (2019) 555–564.
- [46] N. Mahnam, M.H. Beheshty, M. Barmar, M. Shervin, Modification of dicyandiamide-cured epoxy resin with different molecular weights of polyethylene glycol and its effect on epoxy/glass prepreg characteristics, *High Perform. Polym.* 25 (2013) 705–713.
- [47] F. Tikhani, M. Jouyandeh, S.H. Jafari, S. Chabokrow, M. Ghahari, K. Gharanjig, F. Klein, N. Hampp, M.R. Ganjali, K. Formela, M.R. Saeb, Cure Index demonstrates curing of epoxy composites containing silica nanoparticles of variable morphology and porosity, *Prog. Org. Coat.* 135 (2019) 176–184.
- [48] M. Jouyandeh, O.M. Jazani, A.H. Navarchian, M. Shabaniyan, H. Vahabi, M.R. Saeb, Surface engineering of nanoparticles with macromolecules for epoxy curing: development of super-reactive nitrogen-rich nanosilica through surface chemistry manipulation, *Appl. Surf. Sci.* 447 (2018) 152–164.